Brilliance
Research of Artificial Intelligence

E-ISSN : 2807-9035
Volume 4, Number 2, November 2024
https://doi.org/10.47709/brilliance.v4i2.5164

Accelerating the Identification of Soil Drought Index in Wair Koja Village Using Web-Based Thornthwaite-Mather Water Balance Calculations

Margaretha Yuneta[1*], Maria Kurniaty Lete[2], Maria Wihelmina Lodan[3]
[1,2,3]Universitas Nusa Nipa, Indonesia
[1]maragrethayuneta22@gamil.com, [2]atilete@gmail.com, [3]lodanmarina@gmail.com

open access

***Corresponding Author**

Article History:
Submitted: 03-12-2024
Accepted: 18-12-2024
Published: 26-12-2024

Keywords:
drought; drought index; wairkoja village; thornthwaite-mather water balance; website.

ABSTRACT

Wairkoja Village is one of the villages in the Kewapante Sub-district, Sikka Regency, where drought issues have been identified in several areas of agricultural land. A survey conducted on-site revealed extremely dry soil conditions, and the main crop, maize, had dried up or failed to yield. This research is highly urgent to address the drought problem in the study area. Through this research, it is possible to evaluate drought events, including the drought index, the impact of drought on the economic growth of residents, recommendations for addressing drought issues, and educational information regarding the drought index through web-based digital media. The purpose of this study is to provide information about the drought index at the study location using the Thornthwaite-Mather water balance method and to offer recommendations to farmers regarding the impacts of drought problems (crop failure) based on the levels of the drought index. Additionally, it aims to develop a drought index calculation website using the Thornthwaite-Mather water balance method to deliver information about drought issues in specific areas. This research employs ArcGIS software to analyze data, including soil type maps, land use maps, and topographic maps of the study area. The outputs of this research will provide information on the drought index in the study location using the web-based Thornthwaite-Mather water balance method. This study is classified as basic research with Technology Readiness Level (TRL) 2: formulation of concepts and/or technological applications.

INTRODUCTION

Drought is one of the natural disasters that has a long-term impact on the economy of residents and the survival of living beings. Drought occurs due to reduced rainfall, leading to an imbalance in water availability for food crops. The lack of water availability causes food crops to fail. According to reports, the Department of Agriculture in Sikka Regency, East Nusa Tenggara, reported that 24.5 hectares of land planted with corn in the area failed to produce due to the effects of drought, with severe damage occurring in Kangae District, covering 142 hectares. This district, which is adjacent to Kewapante District, suffers from drought issues in both areas. (Jehadu & Kurniati, 2024).

This study identifies the drought index using the Thornthwaite-Mather method, provides practical recommendations for addressing crop failure based on drought levels, and develops a web-based system to analyze and visualize the results of the drought index (Adi et al., 2021), (Laimeheriwa et al., 2020). The focus of this research involves numerical aspects with a civil engineering approach, which is relevant for providing data-based solutions to issues such as drought, crop failure, and their impact on food production. This study aims to address the urgent problems at the study location by determining the level of drought using the Thornthwaite-Mather method, developing mitigation and adaptation measures that can be implemented by farmers to reduce the impact of crop failure, and advancing its application through a web-based platform. Problems encountered at the research site include natural disasters such as recurring drought events from 2021 to 2024 (Zulilmi & Yoseph CSSSA, 2021). These drought events have impacted the residents' economy and livelihoods, forcing those who work as farmers to take up side jobs as livestock keepers and woven fabric artisans (Aalimah et al., 2022).

Proposed solution: The research team aims to identify the soil drought index in Wairkoja Village after the occurrence of soil drought. A failed harvest area will be sampled for calculating the drought index using the Thornthwaite-Mather water balance method. Using the Thornthwaite Mather water balance method, we will obtain the water surplus (water availability) and water deficit (water shortage) values and determine the level of drought (Aalimah et al., 2022). After using the Thornthwaite Mather water balance method, the researcher will then find out the level of the index (Pramesti et al., 2020). By using the Thornthwaite-Mather water balance method, we can obtain the values of water surplus (water availability) and water deficit (water shortage) and determine the level of drought severity. After applying the Thornthwaite-Mather water balance method, researchers will identify the magnitude of the drought index at the study location and provide recommendations or solutions to farmers to address the impacts of drought, such as crop failure (Akhbar et al., 2023), (Dewantara & Munawar Ali, 2023). his crop failure can be addressed by choosing

Brilliance
Research of Artificial Intelligence

E-ISSN : 2807-9035
Volume 4, Number 2, November 2024
https://doi.org/10.47709/brilliance.v4i2.5164

alternative options to avoid the impact of drought, such as planting crops that are adjusted based on index calculations, specifically the amount of water content available. Additionally, the drought index calculations using the Thornthwaite-Mather water balance method are inputted into a website at each stage, enabling the calculations to be performed with the help of the website. Furthermore, the website will also be developed to analyze the impact of specific soil drought index levels on food commodity yields (considering food prices, area size, years, and index comparisons) (Perdinan et al., 2023).

LITERATURE REVIEW

Research on drought shows that drought is a complex phenomenon involving interactions between climate, soil, and human activities. Drought indices are used to measure and map the level of drought in a region, with various approaches, such as meteorological, agronomic, and hydrological (Perdinan et al., 2023). The Thornthwaite-Mather approach, based on the water balance, is one of the methods commonly used to model water availability in the soil because it can combine data on rainfall, evapotranspiration, and groundwater reserves (Nandini & Kusumandari, 2022). The literature review shows that this method provides more accurate results in determining water deficits and surpluses compared to simple statistical methods, especially in tropical areas with seasonal rainfall patterns.

The water balance according to Thornthwaite-Mather is based on the calculation of potential evapotranspiration (PET) which takes into account factors such as air temperature and soil physical properties This method simplifies the analysis of water dynamics in soil, which is relevant for identifying drought indices on a local scale, such as in Wair Koja Village (Chairunnisa et al., 2021). Previous studies have successfully utilized this method to map drought in various tropical regions, such as East Java and East Nusa Tenggara, where the analysis results are often used to support decision-making in water resource management (Uspessy et al., 2020).

The advancement of information technology enables the automation of environmental data analysis through web-based applications. Research shows that integrating the Thornthwaite-Mather water balance into a web-based GIS (Geographic Information System) application can accelerate drought data analysis, improve data accessibility, and facilitate decision-making at the local level. Successful implementation examples include web-based drought disaster monitoring applications that use real-time data from automatic weather stations. Literature studies emphasize the importance of user-friendly interfaces and integration with spatial data to provide fast and accurate information to users, particularly farmers and local governments.

The advancement of information technology enables the automation of environmental data analysis through web-based applications. Research shows that the integration of the Thornthwaite-Mather water balance into a web-based Geographic Information System (GIS) application can accelerate drought data analysis, enhance data accessibility, and simplify decision-making at the local level (Barung & Pattipeilohy, 2020). Successful implementation examples include web-based drought monitoring applications that use real-time data from automatic weather stations. Literature studies emphasize the importance of user-friendly interfaces and integration with spatial data to provide fast and accurate information to users, especially farmers and local governments.

A local study conducted in areas with characteristics similar to Wair Koja Village revealed that semi-arid tropical regions like this are highly vulnerable to drought. Uneven rainfall and the soil's ability to store water are key factors in the water balance analysis. Previous research highlighted that slow environmental data management can exacerbate the impact of drought on the agricultural sector. Therefore, accelerating drought identification through web-based modeling has become a practical solution for regions like this.

Various studies support that the Thornthwaite-Mather method can be effectively used to analyze soil drought indices, especially in tropical regions (Pamungkas & Andika, 2021), (Salehudin et al., 2022). With integration into a web-based system, the process of drought identification becomes faster, more accurate, and accessible to various parties. Literature studies emphasize the importance of automation and web-based technology in supporting drought management at the local level, such as in Wair Koja Village, to address climate change challenges and the need for sustainable water management.

METHOD

The method used in this study, which focuses on accelerating the identification of soil drought index in Wairkoja Village, employs the Thornthwaite Mather water balance calculation method. The Thornthwaite Mather method is used to calculate potential evapotranspiration based on monthly temperature data. This process helps assess the atmosphere's capacity to evaporate water from the soil and vegetation. The analysis of water storage capacity is conducted by utilizing GIS software to combine Thiessen polygon maps, land use maps, and soil texture maps. This process provides the average water storage capacity value for the study area. The analysis is conducted to identify the months with kekurangan atau The advantages of water, shortages, or surplus are calculated from the difference between precipitation and potential evapotranspiration, measured monthly. This index is determined by calculating the proportion of water deficit to potential evapotranspiration. Drought severity levels (light, moderate, severe) are assigned based on the index value. This approach combines primary data (such as temperature and rainfall) and secondary data (such as land maps and land use), enabling more accurate identification of drought conditions.

Brilliance
Research of Artificial Intelligence

E-ISSN : 2807-9035
Volume 4, Number 2, November 2024
https://doi.org/10.47709/brilliance.v4i2.5164

The stages in this study are as follows, the stages of calculating the drought index using the Thornthwaite-Mather method using references (Aripbilah & Suprapto, 2021) and (Lias et al., 2020) while website-based drought index planning uses references (Ermilinda et al., 2023):

1) Enter the average rainfall data for the area for 10 years from January to December.
2) Find the heat index value (I), the Heat Index (I) is the sum of the monthly heat index values (i) calculated using the formula $i = \left(\frac{T}{5}\right)^{1,514}$ (1)
   Description: The T value is the monthly temperature value.
3) Find the ETP before correction (ETPx) Calculate the potential evapotranspiration before correction using the formula: $ETPx = 16\left(\frac{10T}{I}\right)^{a}$ (2)
   Information:
   T = Monthly temperature
   $A = (0{,}000000675.I^3)\ (0{,}000077.I^2) + 0{,}01792.I + 0{,}49239$ (3)
   I = Annual heat index
4) Finding ETP after correction (ETP) Corrected ETP is calculated using the formula : *ETP = f x ETPx (3)*
   Description: f = correction factor based on the latitude of the research location.
5) Find the difference between rainfall and corrected ETP. This step is to subtract the amount of CH (rainfall) in a certain month from the ETP in the same month. The condition of water surplus, if a positive value is obtained. (+), but if a negative result is obtained (-) then the condition is a water deficit.
6) Finding the accumulated potential water loss (APWL) APWL is used to determine the potential water loss in dry months. Calculation method: Starting from the P – ETP value which has a negative value, then sequentially added to the next P – ETP value until the last negative P–ETP value.
7) Look for soil water content (KAT). Calculate the KAT value where APWL occurs using the formula :
   $$KAT = TLP + \left[\left[1{,}00041 - \left(\frac{1{,}07381}{AT}\right)\right]^{APWL} XAT\right] (4)$$
   Description: TLP = permanent wilting point, KL = field capacity, and AT (available water) where AT = KL – TLP (5) For KAT where APWL does not occur, then KAT = last KAT + (P-ETP) (6) The KL value will be used if the KAT value exceeds the KL value.
8) Filling in the column of changes in soil water content (ΔKAT) The ΔKAT value for a particular month is obtained from the KAT of that month minus the KAT of the previous month. A positive value indicates a change in soil water content that occurs at CH > ETP (rainy season), the addition stops when ΔKAT = 0 after KL is reached. All CH and some KAT will be evapotranspired if CH < ETP or ΔKAT is negative.
9) Fill in the Actual Evapotranspiration (ETA) column. If CH > ETP then ETA = ETP (7) because ETA reaches its maximum. If CH < ETP then ETA = CH + |ΔKAT| (8), because all CH and ΔKAT will be evaporated.
10) Filling in the Deficit column (D) Deficit means a reduction in water for evapotranspiration so that D = ETP – ETA (9), occurs during the dry season.
11) Filling in the Surplus column (S) Surplus means excess water when CH > ETP so that, S = (CH – ETP) - ΔKAT (10), occurs during the rainy season.
12) Filling the Run-Off column Run-off (RO) is surface flow or run-off. Thornthwaite and Mather (1957) divided RO into two parts: 50% of the current month's surplus (Sn). 50% of the previous month's RO (ROn -1) (11). So, the current month's RO (Rn) = 50% (Sn + Ron-1) (12) Especially for January's RO, because ROn-1 has not been filled, ROn-1 is taken as 50% of the December surplus.
13) Calculate Ia, the presentation of the drought index using the equation. $Ia = \frac{Defisit\ (D)}{Evapotranspirasi\ potensial\ (ETP)} \times 100\%$ (13) Next, we will know the category of drought index, if the value of the drought index gets a value of less than 16.77% then it is said to be a mild or non-existent drought; if the value of the drought index gets value of 16.77-33.33% then it is said to be a moderate drought; if the value of the drought index becomes a value greater than 33.33% then it is said to be a high drought level.
14) Creating a drought index using the Thornthwaite Mather water balance method based on the website
15) Drawing conclusions and suggestions

RESULT

Data Presentation

The results of this research show that the research team obtained both primary and secondary data. The primary data was obtained from the BMKG website account, which includes monthly rainfall data and monthly temperature data for the past 10 years, as well as coordinate and elevation data of the rain stations. Meanwhile, the secondary data was obtained through data processing using ArcGIS software, which includes soil classification maps, research location maps, and land use area data of the study location. The data collection period for this research was 2 weeks. The obtained primary and secondary data are presented in Tables 1-4 and Figures 1-4 below.

Brilliance
Research of Artificial Intelligence

E-ISSN : 2807-9035
Volume 4, **Number** 2, November 2024
https://doi.org/10.47709/brilliance.v4i2.5164

Table 1 rainfall data from Fransiskus Xaverius Seda Station shows the variation in total annual rainfall from 2014 to 2023. The year with the highest rainfall was 2021, with a rainfall value of 449.8 millimeters per year, while the lowest year was 2015, with a rainfall value of 198.3 millimeters per year. Monthly rainfall is not evenly distributed throughout the year. Months such as June to September often record low or zero rainfall, indicating the dry season, while November and December tend to have higher rainfall, indicating the rainy season.

Table 1. Rain Data for Fransiskus Xaverius Seda Station Year 2014-2023

No	year	Month												SUM
		Jan	Feb	Mar	Apr	May	Jun	Jul	Aug	Sep	Oct	Nov	Dec	
1	2014	54.1	40.5	41	28.5	3.0	0.5	8.5	0	0.0	0.0	0	27.2	203.3
2	2015	43.3	57.9	40.7	7.9	7.9	2.0	0.0	0	0.1	0.0	14.9	23.6	198.3
3	2016	70	34.5	29	16.8	42.5	55.5	21.5	8.9	25.6	12.0	15.4	59.9	391.6
4	2017	50.7	24.2	34	110.4	6.5	0.0	2.0	3.5	13.5	6.6	35.2	25.7	312.3
5	2018	29.7	85.6	27.2	10	0.0	0.0	0	11.2	0.5	21.6	17	76.9	279.7
6	2019	64.5	70.4	22.8	24.2	7.4	4.0	0	0	0.0	12.5	17	29	251.8
7	2020	23.2	27.9	23.1	53	53.0	14.6	0	0.4	0.0	8.5	15.4	47	266.1
8	2021	55.4	120	37.5	32	0.0	8.5	0	7.5	19.7	22.7	90.5	56	449.8
9	2022	24.3	42.4	80.4	20.2	6.0	74	13	0	8.9	18.5	75.8	71.1	434.6
10	2023	65	55.4	13.6	30.2	1.0	30	24.3	0.2	0.0	1.0	16.4	49	286.1

Table 2 presents the latitude, longitude, and evaluation coordinate data. The location of Fransiskus Xaverius Seda rain post is located at latitude coordinates -8.63577 and longitude 122.23752. and this post is at an elevation of 28 meters above sea level.

Table 2. Coordinates and Elevation Data of the Rain Station

Rain post	LATITUDE	LONGITUDE	ELEVATION
Fransiskus Xaverius Seda	-8.63577	122.23752	28

Table 3 shows that in general, rainfall varies between months and years. The highest rainfall tends to occur in May to June, while lower rainfall often occurs in August and September.

Table 3. Rain Data for Fransiskus Xaverius Seda Station

Year	Jan	Feb	Mar	Apr	May	Jun	Jul	Aug	Sep	Oct	Nov	Dec
2014	24	24	24	24	24	25	25	19	16	20	20	19
2015	14	24	24	25	23	23	25	22	23	20	25	26
2016	23	23	24	24	26	23	24	24	25	25	25	25
2017	24	22	23	23	24	24	23	23	22	25	24	24
2018	20	22	22	24	25	24	23	22	21	22	21	22
2019	25	25	25	25	25	23	23	21	22	24	25	26
2020	25	23	25	25	25	22.8	23	23	27	24	26	23
2021	24	24	23	23	24	23	23	23	25	26	25	25
2022	25	24	23	25	25	24	23	23	25	25	25	24
2023	24	24	24	24	24	23	24	22	21	22	25	26

Brilliance
Research of Artificial Intelligence

E-ISSN : 2807-9035
Volume 4, **Number** 2, November 2024
https://doi.org/10.47709/brilliance.v4i2.5164

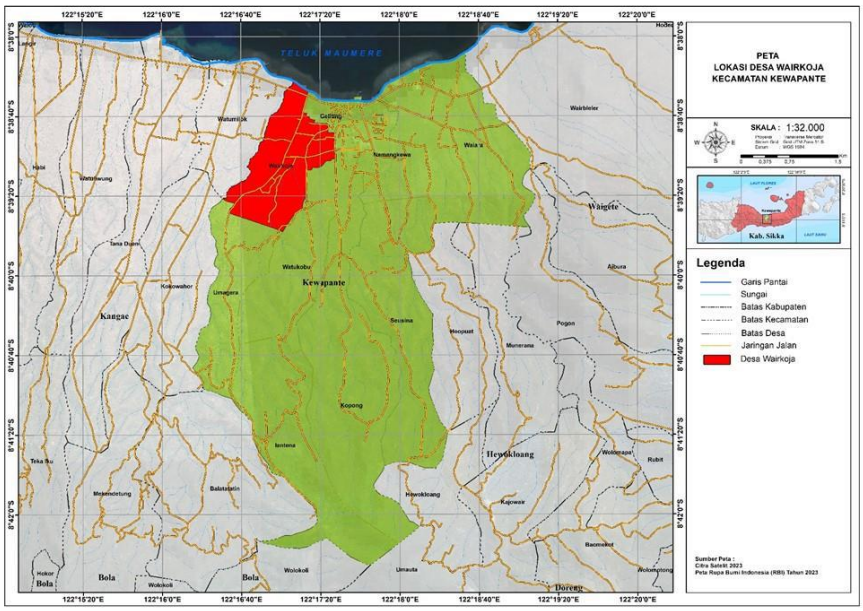

Figure 1: Map of the Research Location

The image above is a map of the location of Wairkoja Village, Kewapante District, with a scale of 1:32,000. This map shows the Wairkoja Village Area (marked in red), located in the northern part of Kewapante District, close to the coastline of Maumere Bay. The map is equipped with elements such as road networks, village boundaries, sub-district boundaries, district boundaries, rivers, and coastlines, which provide a geographical overview and accessibility of the area.

Table 4. Data on Land Use Area of the Research Location

POINT	Shape	Classification of shapes	SOIL TYPE	LAND COVER	LAND TYPE	AREA PER SQUARE METER
0	Polygon ZM	Va.116-n	Ustik Cambisol	Settlements and Places of Activity	Silty Clay & Sand	29,180 sq m
1	Polygon ZM	Va.115-b	Mollisol Ustik	Settlements and Places of Activity	Clay Loam	9,755 sq m
2	Polygon ZM	Va.116-n	Ustik Cambisol	Settlements and Places of Activity	Silty Clay and Sand	0,673 sq m
3	Polygon ZM	Va.116-n	Ustik Cambisol	Settlements and Places of Activity	Silty Clay and Sand	14,694 sq m
4	Polygon ZM	Va.116-n	Ustik Cambisol	Field	Silty Clay and Sand	4,320 sq m
5	Polygon ZM	Va.115-c	Mediterranean Ustik	Plantation	Dusty Clay	215,345 sq m
6	Polygon ZM	Va.115-c	Mediterranean Ustik	Field	Dusty Clay	24676,089 sq m
7	Polygon ZM	X.1	Escarpments	Settlements and Places of Activity	clay loam	63823,165 sq m
8	Polygon ZM	X.1	Escarpments	Settlements and Places of Activity	clay loam	12190,198 sq m
9	Polygon ZM	X.1	Escarpments	Field	clay loam	83,539 sq m
10	Polygon ZM	Va.115-c	Mediterranean Ustik	Field	Dusty Clay	50267,829 sq m
11	Polygon ZM	Va.116-n	Ustik Cambisol	Plantation	Silty Clay and Sand	3989,237 sq m
12	Polygon ZM	Va.116-n	Ustik Cambisol	Plantation	Silty Clay and Sand	245,782 sq m
13	Polygon ZM	Va.116-n	Ustik Cambisol	Plantation	Silty Clay and Sand	998,421 sq m
14	Polygon ZM	Va.116-n	Ustik Cambisol	Plantation	Silty Clay and Sand	1149,181 sq m
15	Polygon ZM	Va.116-n	Ustik Cambisol	Plantation	Silty Clay and Sand	4209,761 sq m
16	Polygon ZM	Va.116-n	Ustik Cambisol	Field	Silty Clay and Sand	45324,945 sq m
17	Polygon ZM	Va.116-n	Ustik Cambisol	Settlements and Places of Activity	Silty Clay and Sand	64475,973 sq m
18	Polygon ZM	Va.116-n	Ustik Cambisol	Settlements and Places of Activity	Silty Clay and Sand	104825,282 sq m
19	Polygon ZM	Va.116-n	Ustik Cambisol	Settlements and Places of Activity	Silty Clay and Sand	167808,812 sq m
20	Polygon ZM	Va.116-n	Ustik Cambisol	Field	Silty Clay and Sand	464213,816 sq m
21	Polygon ZM	Va.115-b	Mollisol Ustik	Plantation	clay loam	48735,661 sq m
22	Polygon ZM	Va.115-b	Mollisol Ustik	Settlements and Places of Activity	clay loam	2158,497 sq m
23	Polygon ZM	Va.115-b	Mollisol Ustik	Settlements and Places of Activity	clay loam	62510,005 sq m
24	Polygon ZM	Va.115-b	Mollisol Ustik	Plantation	clay loam	88372,048 sq m
25	Polygon ZM	Va.115-b	Mollisol Ustik	Field	clay loam	692418,695 sq m

Brilliance
Research of Artificial Intelligence

E-ISSN : 2807-9035
Volume 4, Number 2, November 2024
https://doi.org/10.47709/brilliance.v4i2.5164

Data Analysis

The calculation of the Drought Index using the Thornthwaite-Matter Method.

Analysis of Potential Evapotranspiration

Potential evapotranspiration (PE) is the total ability of the air to carry out evaporation when the moisture supply for vegetation is unlimited. The potential evapotranspiration for each month is calculated using the Thornthwaite Mather method, as presented in the following table 5.

Table 5 Evapotranspiration Thornthwaite Mather Method, Fransiskus Xaverius Seda Station in 2014

Month	T (°C)	i	I	α	*PEX* mm/month	*f*	PE mm/month
Jan	24.39	11.01	113.50	2.526365	110.47	1.008	111.357
Feb	23.61	10.48			101.76	0.954	97.086
Mar	23.90	10.68			105.02	1.030	108.170
Apr	24.33	10.98			109.86	1.008	110.732
May	24.39	11.01			110.47	1.036	114.447
Jun	24.60	11.16			112.93	0.994	112.224
Jul	24.60	11.16			112.93	1.036	116.995
Aug	19.16	7.64			60.07	1.026	61.623
Sep	16.03	5.84			38.29	0.998	38.214
Oct	19.84	8.06			65.58	1.042	68.335
Nov	20.03	8.18			67.22	1.002	67.359
Dec	18.58	7.30			55.58	1.056	58.690

Description of table 5, the first column of months shows the number of months in a year, the second column of T value indicates the number of air temperatures in degrees Celsius in 2014, the third column of i value shows the results of the heat index calculation, the fourth column of I value shows the heat index value during 2014, the fifth column of α value shows the results of the heat index calculation, the sixth column of PEX value shows the potential evapotranspiration value has not been corrected (mm/month), the seventh column of f value shows the correction factor value, this correction value is seen in the latitude and time correction table, the eighth column of PE value shows the corrected potential evapotranspiration (mm/month), based on table 5 shows that in July has the largest corrected potential evapotranspiration value, which is 116,995 mm/month, this is because in that month it has the largest air temperature value of 24.60 degrees Celsius so that it affects the corrected potential evapotranspiration value.

Table 6. Evapotranspiration Method Thornthwaite Mather Station Fransiskus Xaverius Seda year 2015

Month	T (°C)	i	I	α	*PEX* mm/month	*f*	PE mm/month
Jan	13.55	4.52	119.00	2.624881	22.49	1.008	22.671
Feb	24.07	10.80			101.67	0.954	97.000
Mar	24.29	10.95			104.12	1.030	107.242
Apr	24.50	11.09			106.49	1.008	107.340
May	22.97	10.06			89.89	1.036	93.122
Jun	23.03	10.10			90.56	0.994	90.001
Jul	24.60	11.16			107.64	1.036	111.517
Aug	21.65	9.19			76.93	1.026	78.919
Sep	22.63	9.84			86.49	0.998	86.316
Oct	19.77	8.02			60.68	1.042	63.227
Nov	25.03	11.46			112.69	1.002	112.923
Dec	25.55	11.82			118.88	1.056	125.534

Based on table 6 shows that in December has the largest corrected potential evapotranspiration value, which is 125.534 mm/month, this is because in that month it has the largest air temperature value of 25.55 degrees Celsius so that it affects the corrected potential evapotranspiration value.

Brilliance
Research of Artificial Intelligence

E-ISSN : 2807-9035
Volume 4, **Number** 2, November 2024
https://doi.org/10.47709/brilliance.v4i2.5164

Table 7. Evapotranspiration Method Thornthwaite Mather Station Fransiskus Xaverius Seda year 2016

Month	T (°C)	i	I	α	*PEX* mm/month	*f*	PE mm/month
Jan	22.97	10.06	130.82	2.836726	78.98	1.008	79.612
Feb	23.31	10.29			82.37	0.954	78.582
Mar	24.42	11.04			93.98	1.030	96.796
Apr	23.70	10.55			86.33	1.008	87.020
May	25.71	11.93			108.76	1.036	112.669
Jun	23.03	10.10			79.62	0.994	79.127
Jul	23.97	10.73			89.13	1.036	92.341
Aug	23.68	10.53			86.10	1.026	88.327
Sep	24.73	11.25			97.45	0.998	97.245
Oct	25.32	11.66			104.18	1.042	108.551
Nov	25.13	11.53			101.98	1.002	102.195
Dec	24.61	11.17			96.11	1.056	101.488

Based on table 7 shows that in May has the largest corrected potential evapotranspiration value, which is 112.669 mm/month, this is because in that month it has the largest air temperature value of 25.71 degrees Celsius so that it affects the corrected potential evapotranspiration value.

Table 8. Evapotranspiration Method Thornthwaite Mather Station Fransiskus Xaverius Seda year 2017

Month	T (°C)	i	I	α	*PEX* mm/month	*f*	PE mm/month
Jan	24.19	10.88	124.04	2.715155	98.15	1.008	98.939
Feb	21.89	9.35			74.83	0.954	71.390
Mar	23.06	10.12			86.21	1.030	88.795
Apr	23.00	10.08			85.56	1.008	86.235
May	23.71	10.55			92.91	1.036	96.256
Jun	24.40	11.02			100.44	0.994	99.820
Jul	23.00	10.08			85.56	1.036	88.638
Aug	22.90	10.01			84.58	1.026	86.769
Sep	21.93	9.38			75.21	0.998	75.052
Oct	24.77	11.28			104.68	1.042	109.078
Nov	23.67	10.52			92.46	1.002	92.650
Dec	24.00	10.75			96.04	1.056	101.415

Based on table 8 shows that in October has the largest corrected potential evapotranspiration value, which is 109.078 mm/month, this is because in that month it has the largest air temperature value of 24.77 degrees Celsius so that it affects the corrected potential evapotranspiration value.

Table 9. Evapotranspiration Method Thornthwaite Mather Station Fransiskus Xaverius Seda year 2018

Month	T (°C)	i	I	α	*PEX* mm/month	*f*	PE mm/month
Jan	19.77	8.02	116.66	2.582918	62.53	1.008	63.028
Feb	22.39	9.68			86.21	0.954	82.251
Mar	22.00	9.42			82.36	1.030	84.833
Apr	24.13	10.84			104.60	1.008	105.434
May	24.87	11.35			113.06	1.036	117.129
Jun	24.33	10.98			106.86	0.994	106.193
Jul	22.68	9.87			89.07	1.036	92.282
Aug	22.45	9.72			86.80	1.026	89.044
Sep	21.33	8.99			76.07	0.998	75.913
Oct	22.26	9.59			84.88	1.042	88.445
Nov	21.33	8.99			76.07	1.002	76.228
Dec	21.68	9.21			79.28	1.056	83.719

Based on table 9 shows that in May has the largest corrected potential evapotranspiration value, which is 117.129 mm/month, this is because in that month it has the largest air temperature value of 24.87 degrees Celsius so that it affects the corrected potential evapotranspiration value.

Brilliance
Research of Artificial Intelligence

E-ISSN : 2807-9035
Volume 4, **Number** 2, November 2024
https://doi.org/10.47709/brilliance.v4i2.5164

Table 10. Evapotranspiration Method Thornthwaite Mather Station Fransiskus Xaverius Seda year 2019

Month	T (°C)	i	I	α	*PEX* mm/month	*f*	PE mm/month
Jan	24.70	11.23	129.31	2.809606	98.62	1.008	99.410
Feb	24.60	11.16			97.47	0.954	92.987
Mar	24.75	11.26			99.09	1.030	102.065
Apr	24.67	11.21			98.29	1.008	99.067
May	24.95	11.40			101.47	1.036	105.119
Jun	23.17	10.19			82.34	0.994	81.828
Jul	22.55	9.78			76.31	1.036	79.063
Aug	21.35	9.01			65.50	1.026	67.194
Sep	22.03	9.44			71.52	0.998	71.370
Oct	23.90	10.68			89.91	1.042	93.684
Nov	25.43	11.74			107.03	1.002	107.255
Dec	26.10	12.20			115.06	1.056	121.507

Based on table 10 shows that in December has the largest corrected potential evapotranspiration value, which is 121.507 mm/month, this is because in that month it has the largest air temperature value of degrees 26.10 Celsius so that it affects the corrected potential evapotranspiration value.

Table 11. Evapotranspiration Method Thornthwaite Mather Station Fransiskus Xaverius Seda year 2020

Month	T (°C)	i	I	α	*PEX* mm/ Month	*f*	PE mm/ Month
Jan	25.22	11.59	133.66	2.887495	100.08	1.008	100.879
Feb	23.36	10.32			80.21	0.954	76.522
Mar	25.16	11.55			99.45	1.030	102.435
Apr	25.10	11.50			98.68	1.008	99.462
May	24.93	11.39			96.82	1.036	100.306
Jun	22.80	9.95			74.79	0.994	74.330
Jul	23.38	10.33			80.46	1.036	83.358
Aug	23.40	10.35			80.62	1.026	82.705
Sep	27.27	13.04			125.39	0.998	125.135
Oct	24.47	11.07			91.71	1.042	95.557
Nov	26.15	12.24			111.16	1.002	111.390
Dec	23.38	10.33			80.40	1.056	84.899

Based on table 11 shows that in September has the largest corrected potential evapotranspiration value, which is 125.135 mm/month, this is because in that month it has the largest air temperature value of degrees 27.27 Celsius so that it affects the corrected potential evapotranspiration value.

Table 12. Evapotranspiration Method Thornthwaite Mather Station Fransiskus Xaverius Seda year 2021

Month	T (°C)	i	I	α	*PEX* mm/ Month	*f*	PE mm/ Month
Jan	23.82	10.63	128.06	2.787243	90.22	1.008	90.945
Feb	23.60	10.48			87.96	0.954	83.920
Mar	22.87	10.00			80.59	1.030	83.013
Apr	23.31	10.29			84.95	1.008	85.622
May	23.72	10.56			89.14	1.036	92.344
Jun	22.78	9.93			79.67	0.994	79.178
Jul	22.99	10.07			81.77	1.036	84.718
Aug	23.23	10.23			84.13	1.026	86.303
Sep	24.88	11.35			101.83	0.998	101.625
Oct	25.93	12.08			114.30	1.042	119.100
Nov	24.63	11.18			99.01	1.002	99.213
Dec	24.75	11.26			100.38	1.056	105.999

Based on table 12 shows that in October has the largest corrected potential evapotranspiration value, which is 119.100 mm/month, this is because in that month it has the largest air temperature value of degrees 25.93 Celsius so that it affects the corrected potential evapotranspiration value.

Brilliance
Research of Artificial Intelligence

E-ISSN : 2807-9035
Volume 4, **Number** 2, November 2024
https://doi.org/10.47709/brilliance.v4i2.5164

Table 13. Evapotranspiration Method Thornthwaite Mather Station Fransiskus Xaverius Seda year 2022

Month	T (°C)	i	I	α	*PEX* mm/ Month	*f*	PE mm/ Month
Jan	24.52	11.10	130.97	2.839381	94.93	1.008	95.685
Feb	24.20	10.89			91.50	0.954	87.290
Mar	22.97	10.06			78.88	1.030	81.242
Apr	24.66	11.20			96.44	1.008	97.209
May	24.71	11.24			97.07	1.036	100.560
Jun	23.95	10.72			88.80	0.994	88.248
Jul	23.25	10.25			81.68	1.036	84.618
Aug	23.39	10.34			83.03	1.026	85.181
Sep	24.92	11.38			99.40	0.998	99.193
Oct	25.39	11.70			104.78	1.042	109.178
Nov	24.63	11.18			96.11	1.002	96.311
Dec	24.25	10.92			91.98	1.056	97.129

Based on table 13 shows that in October has the largest corrected potential evapotranspiration value, which is 109.178 mm/month, this is because in that month it has the largest air temperature value of degrees 25.39 Celsius so that it affects the corrected potential evapotranspiration value.

Table 14. Evapotranspiration Thornthwaite Mather Method at Fransiskus Xaverius Seda Station 2023

Month	T (°C)	i	*I*	α	*PEX* mm/ Month	*f*	PE mm/ Month
Jan	24.21	10.89	127.47	2.776714	94.94	1.008	95.703
Feb	24.29	10.95			95.89	0.954	91.480
Mar	24.21	10.89			94.98	1.030	97.828
Apr	24.24	10.91			95.31	1.008	96.066
May	24.31	10.96			96.11	1.036	99.565
Jun	23.41	10.35			86.56	0.994	86.017
Jul	24.00	10.75			92.71	1.036	96.052
Aug	21.63	9.19			69.48	1.026	71.280
Sep	21.47	9.08			68.02	0.998	67.877
Oct	22.39	9.68			76.43	1.042	79.636
Nov	25.36	11.69			108.08	1.002	108.310
Dec	26.00	12.13			115.79	1.056	122.273

Based on table 14 shows that in December has the largest corrected potential evapotranspiration value, which is 122.273 mm/month, this is because in that month it has the largest air temperature value of degrees 26.00 Celsius so that it affects the corrected potential evapotranspiration value.

Analysis of Water Holding Capacity

The calculation of water holding capacity (WHC) at each rain station can be done with the help of ArcGIS software version 10, using the "Geoprocessing" extension to overlay existing spatial data. The estimation of water capacity (WHC) in this study is performed as follows:

1) Thiessen Polygon Map Representation
   The depiction of the Thiessen polygon is obtained by inputting the coordinates and elevation of the rain stations through a table in the Arcview GIS 3.2 software. After the rainfall station distribution map is formed, the Thiessen polygon is created by activating the "CDWR Vector" extension and selecting the "Thiessen Polygon" menu. The spatial data used includes the rainfall station distribution map and the study area map.
2) Land Use Map Representation and Soil Texture Map
   The depiction of land use maps and soil texture does not need to be carried out because spatial data is already in the form of a digitized shapefile. If the spatial data is still in analog form, digitization needs to be performed. Digitization is the process of converting spatial data from analog format into digital spatial data. The digitization process is carried out after scanning each map, then the map is input into Autocad software, followed by digitization by tracing the delineations of the existing analog map. The results of the digitized map are then exported in shapefile format so that they can be displayed in Arcview GIS 3.2 software or ArcGIS.
3) The merging of Polygon Map, Land Use Map, and Soil Texture Map.
   The merging of these three maps is done by overlaying the maps. The overlay is performed by activating the "Geoprocessing" extension, with the selected menu being "Union." From the spatial data resulting from the map merging, the water holding capacity (WHC) is calculated by multiplying the percentage of land use area with the

Brilliance
Research of Artificial Intelligence

E-ISSN : 2807-9035
Volume 4, **Number** 2, November 2024
https://doi.org/10.47709/brilliance.v4i2.5164

available water value and the root zone depth value. The water holding capacity (WHC) value is divided into each Thiessen polygon, so the WHC value used is the average WHC per Thiessen polygon.

Table 15. Land Use Calculation of the Research Location

No.	Land use	SOIL TYPE	Wide		Water is available	Root zone	Dampness
			Square meter	proportion	mm/m	m	mm
1	Settlements and Places of Activity	Silty Clay and Sand	29	0%	200	1.00	0.000335209
2	Settlements and Places of Activity	Clayey Loam	10	0%	250	0.80	0.000112062
3	Settlements and Places of Activity	Silty Clay and Sand	0.673	0%	200	1.00	7.73116E-06
4	Settlements and Places of Activity	Silty Clay and Sand	15	0%	200	1.00	0.000168799
5	Field	Silty Clay and Sand	4	0%	200	1.25	6.20331E-05
6	Plantation	Dusty Clay	215	0%	200	1.50	0.0037107
7	Field	Dusty Clay	24,676	0%	200	1.25	0.354336718
8	Settlements and Places of Activity	Clayey Loam	63,823	0%	250	0.80	0.733175855
9	Settlements and Places of Activity	Clayey Loam	12,190	0%	250	0.80	0.140036284
10	Field	Clayey Loam	84	0%	250	1.00	0.00119958
11	Field	Dusty Clay	50,268	0%	200	1.25	0.721821742
12	Plantation	Silty Clay and Sand	3,989	0%	200	1.50	0.06874022
13	Plantation	Silty Clay and Sand	246	0%	200	1.50	0.004235173
14	Plantation	Silty Clay and Sand	998	0%	200	1.50	0.017204212
15	Plantation	Silty Clay and Sand	1,149	0%	200	1.50	0.019802021
16	Plantation	Silty Clay and Sand	4,210	0%	200	1.50	0.072540161
17	Field	Silty Clay and Sand	45324945.000	3%	200	1.25	650.8443156
18	Settlements and Places of Activity	Silty Clay and Sand	64475973.000	4%	200	1.00	740.6750613
19	Settlements and Places of Activity	Silty Clay and Sand	104825282.000	6%	200	1.00	1204.19233
20	Settlements and Places of Activity	Silty Clay and Sand	167808812.000	10%	200	1.00	1927.722783
21	Field	Silty Clay and Sand	464213816.000	27%	200	1.00	5332.708924
22	Plantation	Clayey Loam	48735661.000	3%	300	0.67	562.655722
23	Settlements and Places of Activity	Clayey Loam	2158497.000	0%	300	0.50	18.59698454
24	Settlements and Places of Activity	Clayey Loam	62510005.000	4%	300	0.50	538.5680855
25	Plantation	Clayey Loam	88372048.000	5%	300	0.67	1020.259856
26	Field	Clayey Loam	692418695.000	40%	250	1.00	9942.797982
Sum total			1,741,005,641	99.99%			21941.160
						Sum Sto	219.412

Land use at the research location presented in Table 15 varies consisting of settlements and activity areas, fields, and plantations that have various types of soil including dusty and sandy clay, clayey clay, and dusty clay. The HWC value obtained from the conversion of land use area using Arcview GIS 3.2 software and data processing is 219,412 mm.

Table 16. Drought Index Value Recap for the Last 10 Years Wairkoja Village Drought Index, Kewapante District

No	Month/Year	2014	2015	2016	2017	2018	2019	2020	2021	2022	2023
1	Jan	51.42	0.00	45.61	29.25	52.88	35.12	77.00	39.08	74.60	32.08
2	Feb	18.71	11.19	25.27	51.64	0.00	23.66	8.00	0.00	49.73	39.37
3	Mar	30.26	26.63	56.01	67.31	8.20	76.05	77.71	5.32	1.01	85.98
4	Apr	74.38	0.00	88.68	80.49	34.07	74.47	75.65	17.48	77.24	68.50
5	May	74.38	16.17	91.48	55.83	61.43	92.04	92.61	48.05	92.44	98.93
6	Jun	85.41	44.73	96.43	44.39	76.86	94.48	94.61	57.38	15.93	65.09
7	Jul	84.76	63.64	99.27	75.73	85.31	99.54	99.99	67.88	83.72	74.68
8	Aug	94.21	73.61	99.52	89.73	78.73	99.67	99.99	74.97	99.24	99.69
9	Sep	95.39	69.10	99.58	65.88	92.38	99.76	100.00	70.61	90.56	99.98
10	Oct	96.38	78.28	99.80	88.99	71.75	86.51	86.92	74.23	82.78	98.73
11	Nov	97.34	62.43	85.31	83.37	74.75	84.05	84.74	8.21	21.24	84.85
12	Dec	52.52	74.58	76.68	40.93	7.88	76.08	65.84	44.49	26.74	59.92

The results of the calculation of the drought index using the Thornthwaite Mather method Thornthwaite Mather shows that at the research location, there has been a drought with a high level of 80%, presented in Table 16, it can be seen that many numbers are colored red over the past 10 years because they have a very high drought index value, while the yellow color indicates a moderate drought index level and the green color indicates a light drought index level.

Recommendations based on the drought index level of the research location

Drought index data over the past 10 years provides powerful insights into drought patterns in Wairkoja Village. The key challenge is how to harness the power of this data to address infrastructure deficiencies and adapt to rapid climate change. There are significant opportunities for developing better water management technologies and programs, but threats related to the environment and climate change cannot be ignored. Proactive action will be needed to mitigate the impact of future droughts.

Brilliance
Research of Artificial Intelligence

E-ISSN : 2807-9035
Volume 4, Number 2, November 2024
https://doi.org/10.47709/brilliance.v4i2.5164

Recommendations regarding suitable plants according to the drought index
Specific recommendations based on the results of the Thornwaite Matter drought index method:

1. For months of severe drought (June to October), it is recommended to plant sorghum, cassava, or peanuts, because these plants can survive in low rainfall conditions.
2. In months with moderate drought (March to May, December), plants such as sweet potatoes, corn, or moringa can be an option because they require less water and are harvested quickly.
3. Long-term crops such as cashew nuts or jackfruit can be planted as a long-term strategy for land utilization affected by severe drought because these plants can survive in dry conditions while producing products of high economic value.
4. With the right plant selection strategy according to the level of drought, areas such as Wairkoja Village can maximize land productivity even when facing the challenge of drought.

Recommendations on the impact of rising food commodity prices on drought disasters :

Severe and recurring droughts in Wairkoja Village over the past 10 years have had a significant impact on food yields and prices. With this understanding, recommendations can be directed at better water management, selection of drought-resistant crop varieties, and efforts to adjust planting schedules. In addition, food pricing and supply policies also need to be considered to reduce the impact of price increases due to reduced production during the dry season.

Planning

On the website for the Acceleration of Identification of Soil Drought Index in Wair Koja Village Using the Thornthwaite-Mather Water Balance Calculation, there are three main menus: Home, Drought Index, and Drought Index Recommendations. Below are the analysis and discussion of the functions and information provided by each menu:

1. Home Menu

This image is a view of the Home page of a website titled "Identification of Soil Drought Index in Wair Koja Village." The Home menu serves as the main page of the website, introducing the goals and benefits of the system. On this page, users are given an overview of the importance of identifying the soil drought index in Wair Koja Village. A brief explanation of the Thornthwaite-Mather method is also included to provide a basicunderstanding of the water balance calculation used in the analysis.Analysis Result : This page's layout is informative and user-education-oriented, helping raise awareness about soil drought issues.

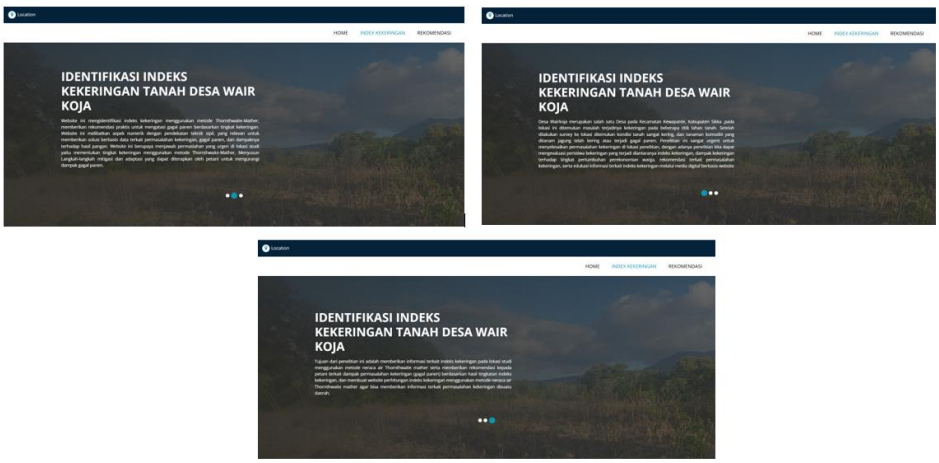

Figure 2. Home Menu

2. Drought Index Menu

This image shows the Drought Index page view on a website. There is a dropdown menu labeled "Select Year." This dropdown allows users to choose data based on a specific year. When a user selects a particular year, the provided information includes input data such as rainfall, potential evaporation, and groundwater balance, as well as output in the form of land drought classification levels. The data is presented in both table and graphical visualization formats to facilitate user interpretation. Analysis Result: The interactive visualization and clear tables make it easier for users, especially local stakeholders, to make data-driven decisions.

Brilliance
Research of Artificial Intelligence

E-ISSN : 2807-9035
Volume 4, **Number** 2, November 2024
https://doi.org/10.47709/brilliance.v4i2.5164

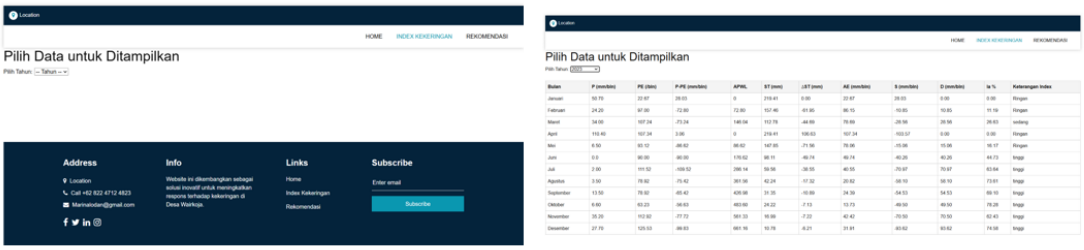

Figure 3. Drought Index Menu

3. Drought Index Recommendation Menu

This image shows the website page for the Drought Index Recommendations section. This menu provides action recommendations based on the results of the drought index classification. The page displays information about the Drought Index, which measures the severity of drought in a specific area. It explains that the drought index is typically grouped into categories such as high, medium, and low for easier understanding. These categories are based on calculation methods, such as the Thornthwaite-Mather Water Balance. There is a "Read More" button, which likely leads users to another page or section for more detailed information.

Figure 4. Drought Index Recommendation Menu

DISCUSSION

The results of the research trial show that the use of the Thornthwaite-Mather water balance method is effective in identifying drought indices in Wair Koja Village. Data processed through ArcGIS software provides detailed information on water surplus and deficit, which are then classified into drought levels. The author's opinion is that integrating this method into a digital-based website not only speeds up the analysis process but also provides broader accessibility to users, including farmers and village governments. However, the accuracy of the results highly depends on the quality of input data, such as rainfall and soil properties, so improving the data collection system should be a focus for future research. Overall, this study has opened up new opportunities for integrated and sustainable drought management.

CONCLUSION

The conclusion of this study is that the drought that occurred in Wairkoja Village, Kewapante District, Sikka Regency, has caused serious losses, including crop failure of maize. This research aims to evaluate the drought event by measuring the drought index, analyzing its impact on the local economy, providing recommendations to farmers, and disseminating information through a website based on the Thornthwaite-Mather water balance method. Using ArcGIS software, land map data, land use, and the earth condition of the research location were analyzed to produce integrated drought index information. This study is expected to provide technology-based solutions to address drought issues and support agricultural sustainability in the area.

ACKNOWLEDGMENT

We would like to express our gratitude to the Ministry of Education, Culture, Research, and Technology for the funding support through the PDP Afirmasi Research Grant, which made this research possible. Our thanks are also extended to the leadership of Higher Education Institutions and the Research and Community Service Institute (LPPM) of Universitas Nusa Nipa for their administrative support and facilities provided throughout the research process. We also appreciate the village of Wairkoja and all parties who have contributed data, information, and cooperation in supporting this research. We hope the results of this study will benefit the sustainable land drought management in Wairkoja Village.

Brilliance
Research of Artificial Intelligence

E-ISSN : 2807-9035
Volume 4, **Number** 2, November 2024
https://doi.org/10.47709/brilliance.v4i2.5164

REFERENCES

Aalimah, R. A., Suryadi, E., & Perwitasari, S. D. N. (2022). Analisis Status Daya Dukung Air Di Sub-DAS Cikeruh berdasarkan Neraca Air Meteorologi Thornthwaite-Mather. *Jurnal Agritechno*, *15*(1), 25–36.

Adi, R. N., Savitri, E., Putra, P. B., & Indrajaya, Y. (2021). Water Balance of Various Peatland Typologies in Central Kalimantan. *IOP Conference Series: Earth and Environmental Science*, *874*(1), 1–10. https://doi.org/10.1088/1755-1315/874/1/012002

Akhbar, A., Naharuddin, N., Kurniadi, R., Malik, A., & Massiri, S. D. (2023). Spatial Distribution of Dryland Forest on Water Availability in Kumaligon Watershed Central Sulawesi, Indonesia. *International Journal of Design and Nature and Ecodynamics*, *18*(2), 369–376. https://doi.org/10.18280/ijdne.180214

Barung, F. M., & Pattipeilohy, W. J. (2020). Neraca Air Lahan dan Tanaman Padi di Kabupaten Manokwari Selatan, Papua Barat pada Tahun 2019. *Buletin GAW Bariri*, *1*(1), 29–36.

Chairunnisa, N., Arif, C., Perdinan, & Wibowo, A. (2021). Analisis Analisis Neraca Air di Pulau Jawa-Bali sebagai Upaya Antisipasi Krisis Air. *Jurnal Teknik Sipil Dan Lingkungan*, *6*(2), 61–80. https://doi.org/10.29244/jsil.6.2.61-80

Dewantara, F. B., & Munawar Ali. (2023). Analisis Potensi Ketersediaan Air Thornthwaite Mather untuk Pengelolaan Sumber Daya Air di Kabupaten Klaten. *Buletin GAW Bariri*, *4*(1), 21–30.

Jehadu, S. S. H., & Kurniati, P. (2024). *24 Hektar Tanaman Jagung di Sikka Gagal Panen.*

Laimeheriwa, S., Madubun, E. L., & Pangguna, M. (2020). Perhitungan Neraca Air Lahan Dan Pemanfaatannya Untuk Penentuan Musim Tanam Di Wilayah Kecamatan Pulau-Pulau Aru, Kabupaten Kepulauan Aru, Provinsi Maluku. *Jurnal Budidaya Pertanian*, *18*(2), 107–115.

Nandini, R., & Kusumandari, A. (2022). Land Use Improvement as the Drought Mitigation to Manage Climate Change in the Dodokan Watershed, Lombok, Indonesia. *Land*, *11*(7), 1–15. https://doi.org/10.3390/land11071060

Pamungkas, G. L., & Andika, Z. K. (2021). Pola Spasial Tingkat Rawan Kekeringan Hidrologis Pada Lahan Padi di Kota Semarang. *Buletin GAW Bariri*, *2*(2), 105–112.

Perdinan, Janna, S. C., Faqih, A., Pratiwi, S. D., & Wibowo, A. (2023). The Contribution of Climate Factors on the Availability of Hydropower Energy in West Java. *IOP Conference Series: Earth and Environmental Science*, *1266*(1), 1–15. https://doi.org/10.1088/1755-1315/1266/1/012059

Pramesti, Debby, Murtini, & Sri. (2020). Analisis daya dukung air meteorik untuk pemenuhan air domestik masyarakat Desa Ngepung, Kecamatan Lengkong, Kabupaten Nganjuk. *Swara Bhumi*, *2*(1), 71–79.

Salehudin, Rohani, Wirahman, L., & Hasyim. (2022). Analisis Indeks Kekeringan Sungai Moyot, Renggung Dan Belimbing Berdasarkan Debit Aliran Sungai. *Jurnal Spektrum Sipil*, *9*(1), 11–18.

Uspessy, J. F., Laimeheriwa, S., & Patty, J. R. (2020). Penentuan Musim Tanam Berdasarkan Perhitungan Neraca Air Lahan di Daerah Saumlaki, Pulau Yamdena. *Jurnal Budidaya Pertanian*, *16*(2), 173–179.

Zulilmi, N. E., & Yoseph CSSSA, B. (2021). Ketersediaan dan Tingkat Kekritisan Air Tanah di Cekungan Air Tanah Labuanbajo, Provinsi Nusa Tenggara Timur. *Padjajaran Geoscience Journal*, *5*(5), 467–476.